IMPROVING THE ACCURACY OF WETLAND MAPPING IN THE ORAN REGION USING LANDSAT DATA AND SVM CLASSIFICATION ENHANCED WITH ADDITIONAL VARIABLES

Sarah Kreri, Yamina Benkesmia, Nezha Farhi

Sarah Kreri
Geomatics science engineer;
Department of Earth Observation,
Center of Space techniques, 31200-Arzew, Oran, Algeria
skreri@cts.asal.dz

Yamina Benkesmia
Hydrogeologist;
Department of Earth Observation,
Center of Space techniques, 31200-Arzew, Oran, Algeria
Department of Geology,
University of Oran 2 Mohamed Ben Ahmed, Georen Laboratory - "Géoressources, Environnement & Risques Naturels", B.P. 1015 El M'naouer, 31000, Oran, Algeria;
yaminabenkesmia@gmail.com

Nezha Farhi
Computer science engineer;
Department of Earth Observation,
Center of Space techniques, 31200-Arzew, Oran, Algeria
nfarhi@cts.asal.dz,

Abstract
Wetland mapping in the region of Oran using medium-resolution Landsat imagery is often affected by spectral confusion. Features such as moist soils, dense aquatic vegetation, urban surfaces, and terrain shadows can easily produce classification uncertainties. To address these limitations, a Support Vector Machine based classification framework was implemented using two Landsat images acquired in 1987 and 2024, representing contrasting spectral conditions. The classification process was conducted in two stages, with and without an optimized training dataset. The enhancement consists of image composition considering seven bands, including original Landsat spectral bands and four supplementary features consiting of spectral indices and texture data. The results demonstrate a substantial improvement in classification performance with the Kappa coefficient values increasing from 0.57 to 0.803in 2024 and from 0.25 to 0.85 in 1987. These findings demonstrate the proposed approach robustness for monitoring spatio-temporal wetland dynamics and supports informed decision-making in the region of Oran.

Keywords*: Wetland mapping; Landsat imagery; Support Vector Machine (SVM); Classification accuracy, Spectral indices.*

INTRODUCTION

Wetlands are among the most productive and most threatened ecosystems on the planet. They provide essential ecological functions such as hydrological regulation, carbon sequestration, biodiversity conservation, and water purification, while being increasingly exposed to growing anthropogenic and climatic pressures. Accurate and regular mapping of these environments is therefore a fundamental prerequisite for their sustainable management and long-term conservation.

Satellite imagery has become a key tool for monitoring and mapping these environments across various spatial and temporal scales. However, this task remains particularly challenging due to the high spatial heterogeneity of wetlands,

their pronounced seasonal dynamics, and the spectral similarities they share with other land cover types, such as irrigated agricultural lands or moist bare soils[1], [2], [3], [4], [5].

These spectral ambiguities represent one of the main sources of error in classifications derived from remote sensing. Recent advances in this field have opened up promising new perspectives. The integration of multi-source data—whether optical, radar, hyperspectral, or LiDAR—combined with the use of machine learning algorithms such as Random Forest, Convolutional Neural Networks (CNN), or Support Vector Machines (SVM), has significantly improved the accuracy of generated maps and enhanced the discrimination between wetland classes.[1], [6], [7], [8], [9].

Similarly, object-based approaches and multi-sensor data fusion methods have shown promising results for large-scale operational mapping[6], [10], [11]. Nevertheless, several challenges remain, including spectral confusion between adjacent classes, difficulties in detecting small wetlands or those obscured by dense vegetation cover, sensitivity to atmospheric conditions, and inherent limitations related to the spatial and temporal resolution of available sensors.[2], [3], [12], [13]

This study is conducted within this context and aims primarily to improve the accuracy of wetland mapping in the Oran region through an original methodological approach designed to reduce spectral confusion between classes. The adopted approach is based on the Support Vector Machine (SVM) algorithm applied to Landsat images acquired in 1987 and 2024, enhanced by the integration of additional variables intended to increase the spectral and spatial separability of land cover classes.

These variables include three Landsat spectral bands (near-infrared, red, and blue), topographic data derived from the SRTM digital elevation model, a textural variable derived from the red band (Data Range), as well as two spectral indices, namely the Normalized Difference Vegetation Index (NDVI) and the PISI built-up index. More specifically, this research pursues three complementary objectives. The first is to evaluate the impact of integrating spectral indices, topographic, and textural variables on the performance of SVM classification. The second aims to analyze the spatio-temporal evolution of wetlands in the Oran region between 1987 and 2024 by comparing the results before and after the enrichment of input data.

The third objective is to produce accurate maps that can support decision-making for the sustainable management and conservation of these environments in a context of increasing human pressure and climate change.

STUDY AREA

The Oran region is located in the north-west of Algeria, approximately 432 km from the capital, Algiers, and covers a total area of 2,114 km² [14] (Figure 1). Its geographical coordinates extend between 1°03' and 0°15' W in longitude and between 35°27' and 35°45' N in latitude. The region is characterized by a semi-arid Mediterranean climate and is distinguished by the presence of several ecologically significant wetland ecosystems, which form an integral component of the natural heritage of north-western Algeria [14].

Three of these wetlands are of exceptional ecological value and benefit from international recognition through their inscription on the Ramsar List of Wetlands of International Importance. Telamine Lake (35°44'09" N; 00°22'57" W), covering an area of 2,399 ha, was designated in 2004. The Great Sebkha of Oran (35°31'29" N; 00°47'12" W), one of the largest salt lakes in Algeria, extending over approximately 56,870 ha, was designated in 2001. The Arzew Saline (35°41'25" N; 00°19'22" W), covering 5,778 ha, were likewise designated in 2004. Together, these three aquatic ecosystems constitute the principal hydrographic entities of the Oran region and represent sites of international importance for biodiversity conservation, particularly as wintering and staging grounds for migratory waterbirds.

Despite their protected Ramsar status, these wetlands are subject to progressive and multifactorial degradation driven by converging anthropogenic pressures, including industrial and domestic pollution, agricultural runoff, accelerated urbanization, and overgrazing [15], [16]. In light of these multifaceted degradation pressures, the systematic cartographic monitoring of these wetland ecosystems has become an urgent scientific and managerial necessity.

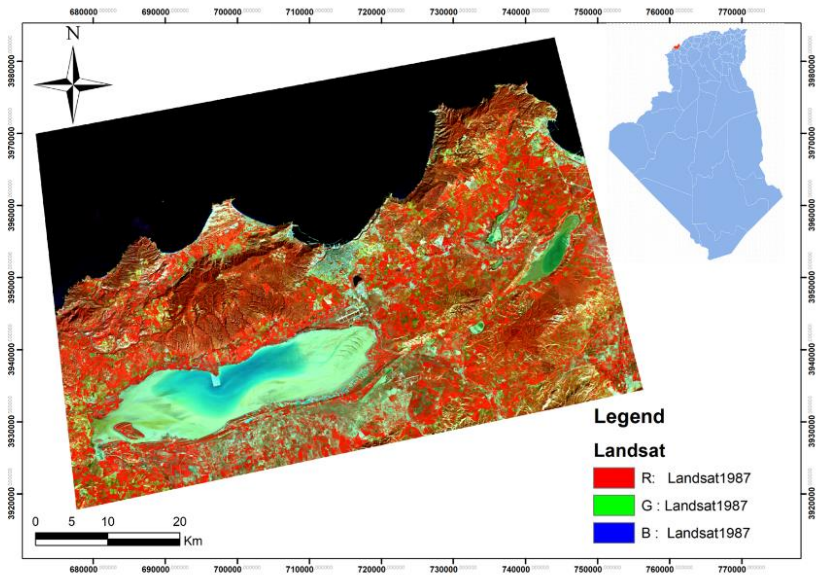

Figure 1. Location of study areas.

METHODOLOGY

This research is grounded in a supervised classification strategy using the Support Vector Machine (SVM) algorithm, with the objective of improving the mapping and representation of wetland areas in the Oran region for the years 1987 and 2024. Landsat satellite imagery was selected for its historical continuity and its spatial resolution, which is well suited to multi-temporal land cover analysis.

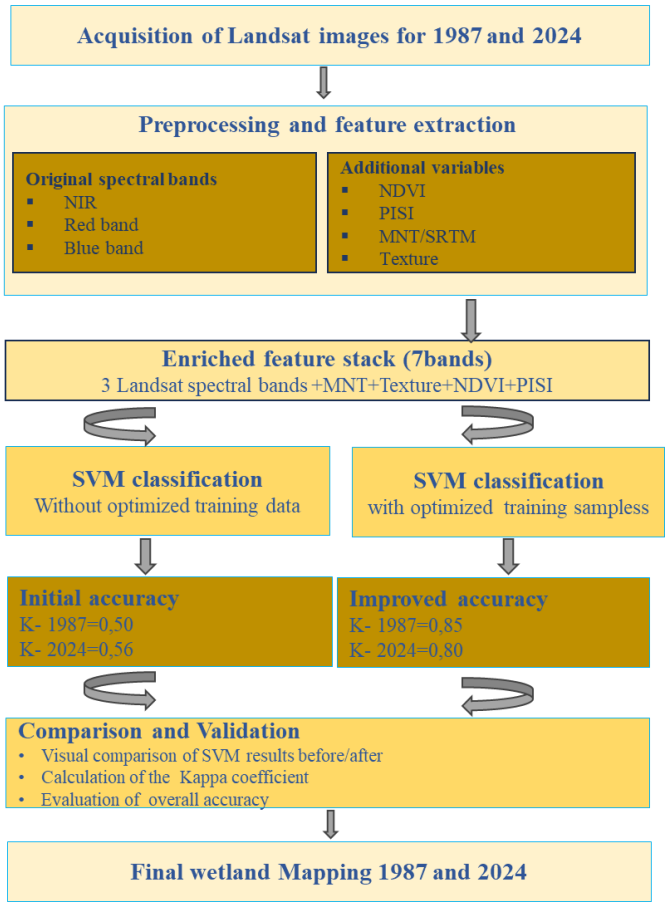

Figure 2. Flowchart of the methodology

Image Preprocessing

Landsat images underwent a rigorous preprocessing workflow to ensure both radiometric and geometric consistency. This phase included radiometric and geometric correction, study area delineation, and the generation of derived variables. These steps were essential to enhance the quality of the input data fed into the classification pipeline.

Classification Algorithm

The SVM algorithm was employed for image classification due to its well-documented effectiveness in handling high-dimensional and non-linear remote sensing data [17], [18]. SVM operates by identifying an optimal hyperplane that maximizes the margin between land cover classes in a multidimensional feature space[19]. This property is particularly valuable in wetland environments, where spectrally similar classes (namely moist soils, saline soils, salt crusts, bare soils, and certain urban surfaces) are prone to confusion.

Feature Composition and Enriched Image Stack

To optimize model performance, classification was applied to an enriched seven-band image composite combining Landsat spectral bands (NIR, Red, Blue)[20], with additional derived variables: the Normalized Difference Vegetation Index (NDVI), the Impervious Surface Index (PISI), the Digital Elevation Model (SRTM), and a texture variable. This multi-source composition significantly enhances the discriminative capacity between spectrally similar classes commonly found in wetland and saline environments.

Classification Design

Two classification scenarios were developed to assess the contribution of supplementary variables in reducing spectral confusion:

- ✓ Scenario 1 (Initial): Classification based solely on the original Landsat spectral bands.
- ✓ Scenario 2 (Optimized): Classification using the full enriched image stack.

Accuracy Assessment

Model evaluation was conducted using a confusion matrix and the Kappa coefficient, enabling a rigorous assessment of overall classification accuracy for both study years. Land cover classes were defined based on their relevance to wetland identification and the spectral confusions observed between surface types in the Oran region.

This methodology (Figure 2) enables a robust spatio-temporal cartographic analysis of wetlands, while substantially improving the reliability and interpretability of the classification results, thereby directly contributing to the fields of GIS and remote sensing-based environmental mapping**.**

RESULTS AND DISCUSSION

Observed Spectral Confusions Before and After the Integration of Additional Variables for 1987

The comparison of the confusion matrices for 1987, before and after the integration of supplementary variables, reveals a substantial improvement in classification performance. The Overall Accuracy increased from 34.35% to 85%, and the Kappa coefficient rose from 0.25 to 0.86 reflecting a marked reduction in inter-class confusion errors.

This level of improvement is consistent with findings reported in the remote sensing literature, where the enrichment of spectral feature spaces through derived indices has been shown to significantly enhance SVM classification accuracy in complex land cover environments, particularly in wetland and semi-arid contexts[19]. To provide a deeper evaluation of classification performance, full confusion matrices were analyzed for the 1987 classifications before and after the integration of supplementary variables (Table 1 and 2). In matrix 1 (Without Variables), 12 classes was identified and the fallow land class shows the highest commission error (74.02%), indicating a strong overestimation due to spectral similarity with other land cover types.

Table 1. Confusion matrix table for the 1987 before the integration of additional variables

Class	Urban	Very wet soil	Wet soil	Open woodland	Clear water	Fallow	Halophytic	Forest	Salt crust	Agriculture	Degraded land	Bare soil
Urban	1093	575	429	0	8	174	3	2	3	0	38	6
Very wet soil	0	0	0	0	0	0	0	0	0	0	0	0
Wet soil	803	32	1468	0	14	244	0	0	20	0	60	36
Open woodland	34	0	4	998	5	161	240	365	0	306	11	0
Clear water	466	319	35	0	553	0	1	0	47	0	0	0
Fallow	1533	1539	414	115	520	2761	131	656	367	24	43	0
Halophytic	0	0	0	0	0	0	0	0	0	0	0	0
Forest	0	0	0	0	0	0	0	0	0	0	0	0
Salt crust	0	0	0	0	0	0	0	0	0	0	0	0
Agriculture	0	0	0	0	0	22	1	0	0	1009	0	0
Degraded land	0	0	0	0	0	0	0	0	0	0	0	0
Bare soil	18	0	0	0	0	0	0	0	0	0	32	139

For the 1987 classification without additional variables (Table 1), an overall accuracy of 34.35% and a Kappa coefficient of 0.25 indicate a severely deficient inter-class discrimination, characterised by the complete failure to detect five out of twelve classes (Very wet soil, Halophytic, Forest, Salt crust and Degraded land), whose pixels are systematically absorbed by the Fallow class, which then acts as the dominant receiving class by erroneously accumulating 1,533 urban pixels, 1,539 Very wet soil pixels, 414 Wet soil pixels, 520 Clear water pixels and 656 Forest pixels, thus revealing the model's discriminative saturation when faced with the spectral proximity of wetland, saline and forest environments in the absence of derived indices, Figure 3.

Table 2. Confusion matrix table for the 1987 after the integration of additional variables

Class	URBAN	Very wet soi	Saline soil	Polluted soil	Wet soil	Open woodl	Fallow3	Clear water	Fallow2	Fallow1	halophyte	Forest	Agriculture	Degraded lar	Bare soil	prairie
URBAN	2233	37	119	22	26	0	111	9	462	378	0	0	0	35	7	0
Very wet soil	718	4618	10	68	549	0	1	6	58	183	0	0	17	2	0	2
Saline soil	12	1	426	0	0	0	117	3	81	12	0	0	0	0	0	3
Wet soil	263	240	78	182	1840	0	1	86	106	19	0	0	0	2	0	0
Open woodland	0	0	0	0	0	1018	9	0	9	25	0	209	3	0	0	0
Fallow3	12	2	77	0	0	0	214	0	19	20	3	0	3	6	0	47
Clear water	16	0	0	92	0	0	0	3426	4	0	5	8	0	0	0	0
Fallow2	378	109	412	21	128	0	84	21	1934	492	7	3	0	9	0	3
Fallow1	380	97	44	36	2	0	107	11	199	2439	10	9	12	12	0	4
halophyte	12	3	0	11	1	39	7	3	8	20	252	24	3	5	0	69
Forest	0	0	0	0	0	68	0	0	2	6	0	767	0	0	0	0
Agriculture	0	0	0	5	0	4	0	6	51	44	6	1	1299	0	0	4
Degraded land	39	0	0	1	0	0	0	0	1	12	0	1	0	103	1	1
Bare soil	10	0	0	0	0	0	0	0	0	0	0	0	0	0	173	0
prairie	15	0	1	0	0	1	27	0	12	6	93	1	2	10	0	159

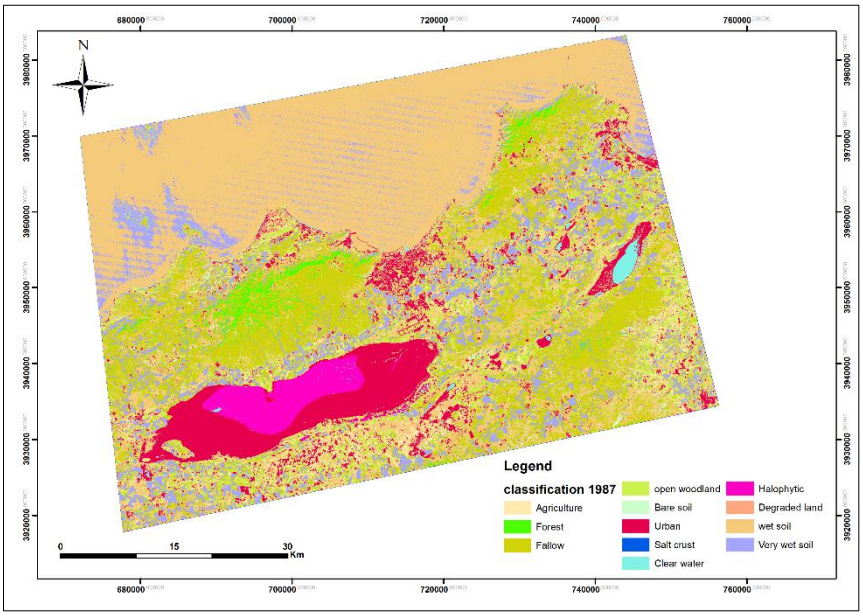

Figure 3. Land use map 1987-without additional data.

.

The inclusion of additional variables for the same period (Table 2) leads to a radical improvement in classification quality, bringing the overall accuracy to 88.52% and the Kappa coefficient to 0.85, with the classification scheme expanded to sixteen classes and the detection of all land cover types restored: the 'Very wet soil' class, previously completely

undetected, now comprises 4,618 correctly classified pixels, whilst 'Forest', 'Halophyte' and the fallow sub-types (Fallow1, Fallow2, Fallow3) become distinguishable thanks to the inclusion of differentiating spectral indices; residual confusion is limited to partial ambiguity between degraded urban areas and wasteland (378 and 462 pixels respectively) as well as between 'Very wet soil' and 'Saline soil' (240 pixels), structural spectral overlaps specific to the sebkha environments of north-western Algeria, Figure 4.

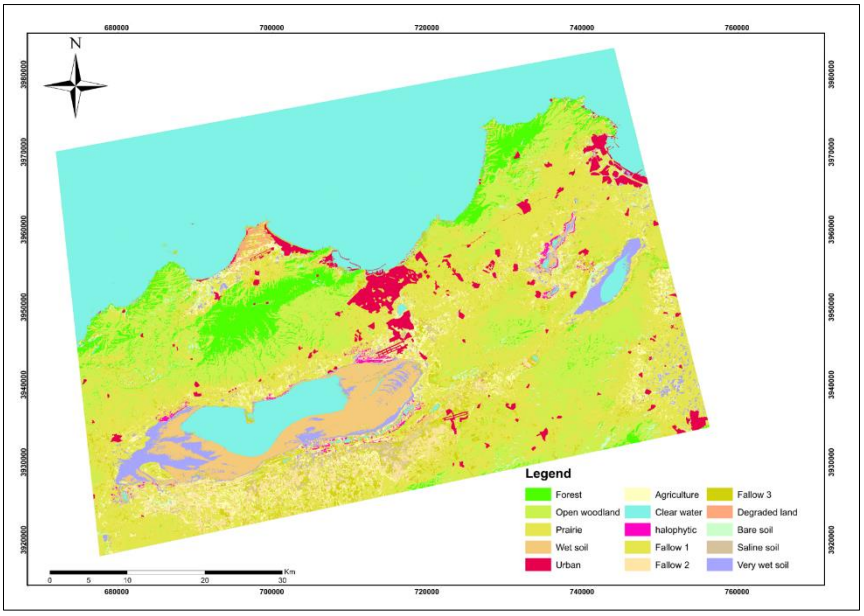

Figure 4. Land use map 1987-with additional data.

Observed Spectral Confusions Before and After the Integration of Additional Variables for 2024

For the year 2024 without additional variables (Table 3), despite a higher overall accuracy than in 1987 (57.01%, Kappa = 0.53), the classification of seventeen classes reveals severe structural confusion affecting, in particular, the classes Bare soil (73 correct pixels), Degraded land (80 pixels), Agriculture (240 pixels) and Dump (224 pixels), anthropogenic and bare-surface classes for which the raw spectral information proves insufficient to distinguish the similar signatures of saline surfaces, fallow land and degraded peri-urban areas, whilst the Fallow1 class once again becomes a source of confusion by absorbing a large number of pixels from the Agriculture, Forest and Saline soil classes.

Table 3. Confusion matrix table for 2024 before the integration of additional variables

Class	Urban	Very wet soil	Saline soil	Polluted soil	Bare soil	Wet soil	Maquis	Fallow3	Mixed water	Clear water	Fallow2	Fallow1	Halophyte	Forest	Agriculture	Dump	Degraded land
Urban	648	56	98	110	24	32	12	85	6	27	137	123	60	14	87	19	34
Very wet soil	112	415	55	0	1	262	0	0	0	7	76	25	21	0	15	31	0
Saline soil	84	4	923	25	3	83	0	2	0	8	294	79	28	0	56	46	0
Polluted soil	35	0	0	569	1	22	63	42	6	22	1	4	26	154	78	0	33
Bare soil	1	0	0	0	73	0	0	9	0	0	21	11	0	0	13	13	3
Wet soil	371	906	125	37	6	2113	3	28	0	25	66	63	56	0	38	58	0
Maquis	56	0	0	329	50	3	1703	142	14	16	5	16	40	433	315	0	51
Fallow3	35	0	0	28	22	25	8	363	6	21	2	10	9	42	49	1	10
Mixed water	0	0	0	5	13	0	1	0	799	4	0	4	10	33	2	0	0
Clear water	9	0	0	0	0	0	0	19	0	1438	0	4	9	2	0	0	0
Fallow2	254	113	247	7	30	60	0	4	0	5	875	160	24	0	30	48	1
Fallow1	162	0	0	3	17	0	0	75	0	4	149	614	11	0	4	11	0
Forest	3	0	0	142	3	0	146	40	10	7	0	3	0	684	20	0	6
Agriculture	28	0	0	18	1	3	42	38	0	9	0	1	10	26	240	0	5
Dump	24	0	0	0	11	0	2	25	0	10	3	33	12	0	15	224	11
Degraded land	13	0	3	0	6	0	33	18	0	1	0	6	15	41	9	11	80

Table 4. Confusion matrix table for the 2024 after the integration of additional variables.

Class	URBAN	Very wet soi	Saline soil	Polluted soil	Bare soil	Wet soil	Open woodl	Fallow3	Mixed water	Clear water	Fallow1	Fallow1	halophytic	Forest	Degraded lar	Agriculture	Dump
URBAN	1605	20	87	8	6	4	4	60	0	12	115	138	33	5	35	28	48
Very wet soi	379	520	99	0	0	418	0	7	0	0	106	2	1	0	2	0	0
Saline soil	99	49	1114	4	0	781	0	3	0	1	730	57	6	0	0	6	0
Polluted soil	0	0	0	505	0	0	6	0	0	0	0	0	12	57	0	64	0
Bare soil	2	0	0	0	800	0	1	0	0	1	5	26	0	0	2	0	82
Wet soil	254	555	151	0	0	2692	0	15	0	0	74	82	9	0	0	2	2
Open woodl	27	0	2	23	0	0	1410	5	0	0	7	4	33	240	6	56	7
Fallow3	138	0	0	12	0	59	4	989	0	1	7	9	9	8	0	13	0
Mixed water	0	0	0	1	0	0	0	0	439	3	0	1	12	3	9	0	0
Clear water	1	0	0	0	0	0	0	0	2	2206	0	0	0	3	12	0	0
Fallow2	230	562	114	3	2	16	0	4	0	0	783	78	5	0	5	2	9
Fallow1	207	31	3	4	15	0	1	29	0	0	198	712	24	0	0	7	43
halophytic	15	0	0	16	0	0	3	4	0	0	1	0	67	29	0	3	0
Forest	10	0	0	92	0	0	238	3	0	1	0	21	31	1078	0	4	1
Degraded lar	39	0	0	1	0	0	0	0	1	12	0	1	0	103	103	1	159
salt crust	82	0	0	0	9	0	0	0	0	3	1	0	0	0	10	0	0
Agriculture	5	0	0	29	0	0	32	2	0	0	2	2	14	3	0	593	0
Dump	24	0	2	1	15	0	3	0	0	0	13	26	1	3	0	0	586

Following the inclusion of additional variables in 2024 (Table 4), the overall accuracy improved to 83.34% (Kappa = 0.82), with notable improvements in the most problematic classes: Bare soil recorded the highest relative gain in the matrix, rising from 73 to 800 correctly classified pixels (a factor of 11), whilst Agriculture (591 pixels), Fallow3 (989 pixels) and Dump (586 pixels) see their performance increase by a factor of 2.5, 2.7 and 2.6 respectively, reflecting the essential contribution of brightness, vegetation and artificiality indices in distinguishing between anthropogenic surfaces and degraded land cover; residual confusion persists mainly between Saline soil and Fallow1 (730 pixels), between URBAN and the sub-types of peri-urban fallow land, as well as between Degraded land and Agriculture or Forest; these ecological ambiguities reflect the spatial and spectral continuity of these themes in transition zones and remain difficult to resolve without the addition of complementary textural, phenological or contextual data, Figure 5.

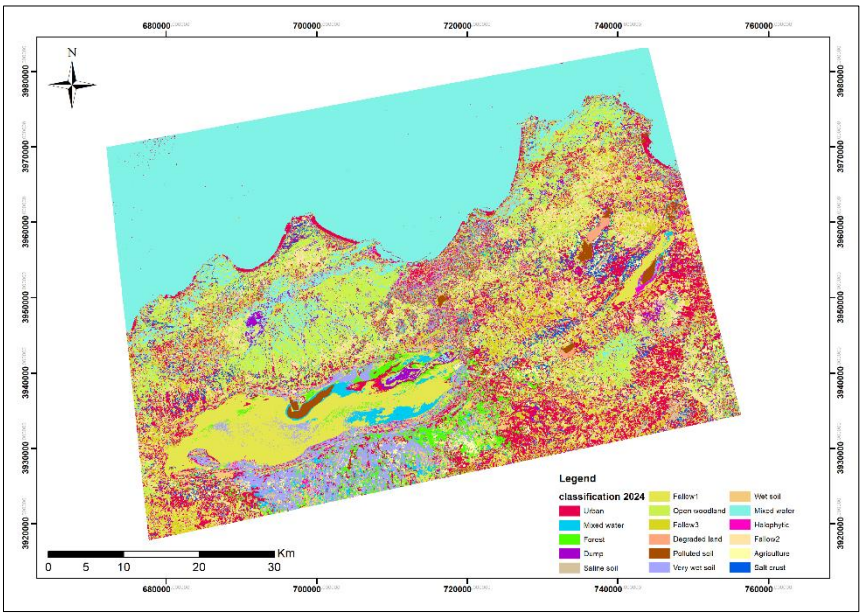

Figure 5. Land use map 2024-without additional data

Overall, the improvement in Overall Accuracy resulting from the additional variables amounts to +54.17 points for 1987 and +26.33 points for 2024, an asymmetry that can be explained by the higher initial classification baseline in 2024 as well as by the increased complexity of a seventeen-class classification scheme, confirming that the enrichment of the spectral space is a necessary, but not sufficient, condition for the reliability of SVM classification in semi-arid environments, and that the reduction of residual confusion requires the complementary integration of structural and temporal variables to achieve the accuracy thresholds demanded by reference thematic mapping standards.

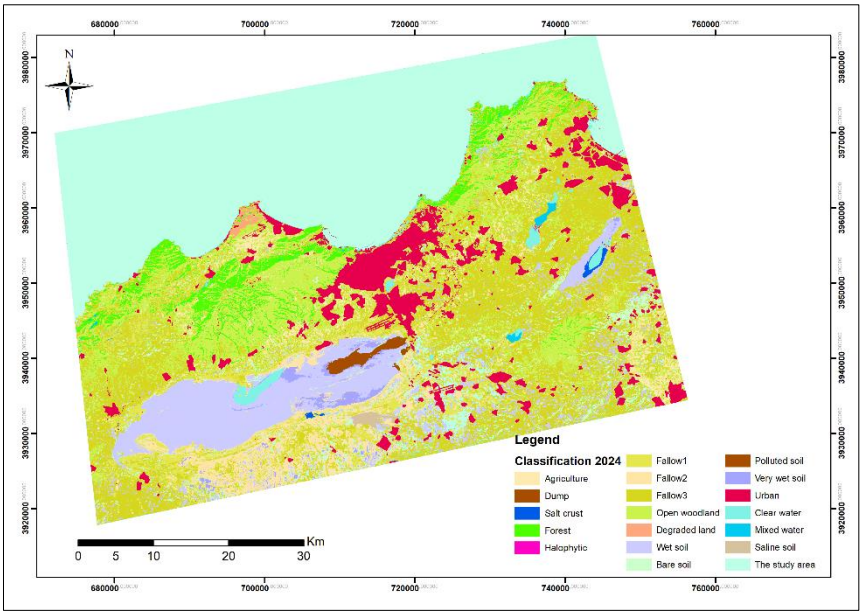

Figure 6. Land use map 2024-with additional data

CONCLUSION

This study assessed the impact of integrating variables from multiple sources on improving land-use classification in wetlands, using Landsat imagery from 1987 and 2024. The exclusive use of the SVM algorithm based on spectral bands revealed certain limitations, mainly due to the spectral similarity between various classes such as wet soils, saline soils, fallow land and urban areas. These misclassifications led to fairly high error rates, as indicated by the Kappa coefficient obtained prior to the integration of additional variables (0.25 for 1987 and 0.53 for 2024). The inclusion of derived variables, such as the NDVI index, the PISI index, textural variables and the DTM, improved the distinction between classes and reduced confusion rates between the different land-use categories. This improvement is reflected in a significant increase in overall accuracy and the Kappa coefficient, reaching 0.85 for 1987 and 0.82 for 2024 respectively, demonstrating a strong agreement between the classifications produced and the reference data.

The results indicate that the integration of derived spectral, textural and topographic variables allows for a better representation of the spatial heterogeneity of wetlands, which are characterised by high environmental variability and the presence of classes exhibiting similar spectral signatures. The approach used helps to better distinguish between wet soils, saline soils, vegetation-covered surfaces and urban areas, thereby minimising spatial changes. The comparative study between 1987 and 2024 highlights the importance of remote sensing and geographic information systems for monitoring the spatio-temporal evolution of land use. The approach presented constitutes a reliable tool for mapping wetlands, promoting a better understanding of their progression over time and the improvement of policies for the management and conservation of these vulnerable ecosystems. For future work, examining the relative importance of additional variables could help assess their individual contribution to improving classification accuracy.

Verifying the hierarchy of impact of these variables would facilitate the selection of the most appropriate parameters. It would also be worthwhile to test other classification algorithms, such as Random Forest or deep learning methods, to assess their performance relative to the SVM algorithm. The integration of multi-temporal data or high-resolution imagery could also improve the detection of classes that still exhibit some confusion.

REFERENCES

[1] X. Zhang *et al.*, « GWL_FCS30: a global 30 m wetland map with a fine classification system using multi-sourced and time-series remote sensing imagery in 2020 », *Earth Syst. Sci. Data*, vol. 15, nº 1, p. 265-293, 2023.

[2] B. Slagter, N.-E. Tsendbazar, A. Vollrath, et J. Reiche, « Mapping wetland characteristics using temporally dense Sentinel-1 and Sentinel-2 data: A case study in the St. Lucia wetlands, South Africa », *Int. J. Appl. Earth Obs. Geoinformation*, vol. 86, p. 102009, 2020.

[3] C. Fan *et al.*, « Mapping phenology of complicated wetland landscapes through harmonizing Landsat and Sentinel-2 imagery », *Remote Sens.*, vol. 15, nº 9, p. 2413, 2023.

[4] D. Mao *et al.*, « National wetland mapping in China: A new product resulting from object-based and hierarchical classification of Landsat 8 OLI images », *ISPRS J. Photogramm. Remote Sens.*, vol. 164, p. 11-25, 2020.

[5] C. Ludwig, A. Walli, C. Schleicher, J. Weichselbaum, et M. Riffler, « A highly automated algorithm for wetland detection using multi-temporal optical satellite data », *Remote Sens. Environ.*, vol. 224, p. 333-351, 2019.

[6] L. Yue, M. Wang, C. Huang, Q. Cheng, Q. Yuan, et H. Shen, « Mapping hierarchical wetland characteristics by optical-SAR integration with collaborative spatial-spectral-temporal learning », *Int. J. Appl. Earth Obs. Geoinformation*, vol. 136, p. 104395, 2025.

[7] W. Sun *et al.*, « A simple and effective spectral-spatial method for mapping large-scale coastal wetlands using China ZY1-02D satellite hyperspectral images », *Int. J. Appl. Earth Obs. Geoinformation*, vol. 104, p. 102572, 2021.

[8] M. Rezaee, M. Mahdianpari, Y. Zhang, et B. Salehi, « Deep convolutional neural network for complex wetland classification using optical remote sensing imagery », *IEEE J. Sel. Top. Appl. Earth Obs. Remote Sens.*, vol. 11, nº 9, p. 3030-3039, 2018.

[9] M. Marjani, M. Mahdianpari, F. Mohammadimanesh, et E. W. Gill, « CVTNet: A fusion of convolutional neural networks and vision transformer for wetland mapping using Sentinel-1 and Sentinel-2 satellite data », *Remote Sens.*, vol. 16, nº 13, p. 2427, 2024.

[10] Y. Cai, X. Li, M. Zhang, et H. Lin, « Mapping wetland using the object-based stacked generalization method based on multi-temporal optical and SAR data », *Int. J. Appl. Earth Obs. Geoinformation*, vol. 92, p. 102164, 2020.

[11] M. Mahdianpari, B. Salehi, F. Mohammadimanesh, S. Homayouni, et E. Gill, « The first wetland inventory map of newfoundland at a spatial resolution of 10 m using sentinel-1 and sentinel-2 data on the google earth engine cloud computing platform », *Remote Sens.*, vol. 11, nº 1, p. 43, 2018.

[12] M. Amani, B. Salehi, S. Mahdavi, et B. Brisco, « Spectral analysis of wetlands using multi-source optical satellite imagery », *ISPRS J. Photogramm. Remote Sens.*, vol. 144, p. 119-136, 2018.

[13] G. Kaplan et U. Avdan, « Evaluating the utilization of the red edge and radar bands from sentinel sensors for wetland classification », *Catena*, vol. 178, p. 109-119, 2019.

[14] M. Ramser, F. Abbassi, M. Pfister, F. Bergfelder, M. A. Puhan, et M. Turina, « Embarking on improvement cycles-the next steps in surgical benchmarking », *Langenbecks Arch. Surg.*, vol. 410, nº 1, p. 298, 2025.

[15] C. Aibeche, W. Sidhoum, A. Djabeur, et M. Kaid-Harche, « Effet des caractéristiques physico-chimiques sur la charge microbienne de l'eau des zones humides du nord-ouest algérien: cas du lac Télamine et de Dayet Oum Ghellaz, Oran », *Algerian J. Environ. Sci. Technol.*, vol. 6, nº 4, 2020.

[16] Y. Benkesmia, M. I. Hassani, et C. Kessar, « Variation of surface water extent in the great Sebkha of Oran (NW of Algeria), using Landsat data 1987–2019: Interaction of natural factors and anthropogenic impacts », *Remote Sens. Appl. Soc. Environ.*, vol. 30, p. 100953, 2023.

[17] C.-N. Lam, « Méthodes de Machine Learning pour le suivi de l'occupation du sol des deltas du Viêt-Nam », 2021.

[18] B. Ibrahim et B. Ameziane, « Machine à vecteur du support (SVM) », 2022.

[19] M. Ndiaye, R. Boissy, et M. Faye, « Évaluation comparative des algorithmes d'apprentissage automatique pour la classification des types de sols à partir de caractéristiques physico-chimiques: application de Random Forest, XGBoost, SVM et KNN », *VertigO- Rev. Électronique En Sci. Environ.*, 2025.

[20] M. Soumia et B. Sofia, « L'évaluation des techniques de sélection des attributs pour la classification du texte arabe », 2023.